POAC'13
Espoo, Finland

Proceedings of the 22nd International Conference on
Port and Ocean Engineering under Arctic Conditions
June 9-13, 2013
Espoo, Finland

Further Improvements to Understandings of Extreme Arctic Sea Ice Thickness Derived From Upward Looking Sonar Ice Data

T.D. Mudge [1], E. Ross [1], D.B. Fissel [1], J.R. Marko [1]
[1]ASL Environmental Sciences Inc., Victoria, CANADA

ABSTRACT

Long-term observations of extreme draft sea ice features have been identified from upward looking sonar (ULS) datasets spanning several years in various Arctic regions including the Canadian Beaufort Sea, offshore of Northeast Greenland and the Chukchi Sea. The quantification of the distribution of magnitude and frequency of occurrence of very deep ice keels is important to the design and strategic deployment plans for offshore platforms and shipping and navigation in these ice covered waters.

An earlier analysis (Amundrud, 2004) led to an empirically determined relationship between the maximum ice draft and the draft of nearby level ice based on draft observations from the Beaufort Sea in the 1990s. It was argued that ridging in first-year ice continues as long as the force required to drive an ice block over the ridge is less than the force at which the level ice next to the ridge will buckle. An empirical upper limit was developed for the maximum sea ice thickness resulting from deformation processes based on the relationship of maximum ice thickness as a function of nearby values of undeformed ice thickness.

Using the more extensive ULS ice keel data sets now available in the Beaufort Sea as well as the NE Greenland and Chukchi Sea areas, these methods were re-evaluated and updated. The results are compared among the regions in terms of the potential source areas for very large ridging activity. The implication of the maximum ice drafts derived in this empirical approach for sea ice ridging are discussed in the context of other ice types that may be present including multi-year ice and floating glacial ice (icebergs and ice islands).

INTRODUCTION

In this paper, we use advanced ULS data sets from widely separated regions in the Arctic Ocean, from the Chukchi Sea area, the Beaufort Sea region (including the Mackenzie Shelf in the Canadian Beaufort Sea and Camden Bay shelf area in E. Alaskan waters) and the Northeast Greenland region (see Figure 1). The ULS data sets span a large range of water depths including shelf waters in depths of 30-100 m and over continental slope regions with depth of greater than 100 m to over 1000 m water depth. This work continues recent research on a subset of these datasets (Ross et al., 2012).

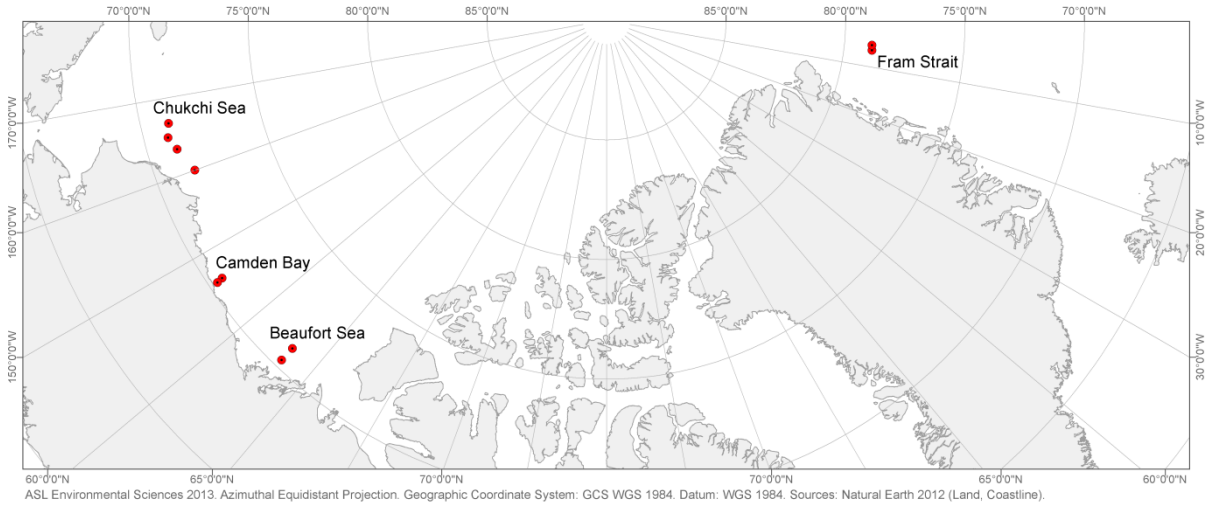

Figure 1. The ULS measurement sites used in this paper.

Ice Profiling

ASL's Ice Profiler (IPS) provides measurements of ice draft and has been used in many ice-covered areas (Fissel et al., 2010; Fissel et al., 2008). The operation of the IPS is depicted in Figure 2. The instrument determines the time-of-flight for the travel of short acoustic pulses from the instrument to a water column target and back to the instrument. The range of the target from the instrument is then calculated using the speed of sound through the water column. A single ping may determine the range to multiple targets. The latest version of the IPS is capable of storing up to five targets per ping and the full profile of the backscattered returns.

Additional sensors on the IPS provide measures of the instrument tilt and pressure enabling conversion of the range measurements to target draft, d, through:

$$d = \eta - \beta \cdot r \cdot \cos\theta \qquad (1)$$

where r is the range to a target, θ is the total instrument tilt, η is the instrument depth and β is a time-dependent correction factor which scales range for variations in the speed of sound. Standard processing methodologies have been developed since 1997 to detect and remove outliers from the range, tilt and pressure data acquired by the IPS.

The β correction factor is empirically determined by identifying episodes of open water which, by definition, have zero draft allowing β to be determined from Equation 1 as:

$$\beta = \frac{\eta}{r \cdot \cos\theta} \qquad (2)$$

The instrument depth is determined by integrating the measured pressure with an independent measure of the atmospheric pressure:

$$\eta = \frac{P_{IPS} - P_{atm}}{\rho g} - \Delta D \qquad (3)$$

where P_{IPS} is the pressure measured by the IPS, P_{atm} is the atmospheric pressure, ρ is the mean density of the seawater above the instrument, g is the local gravitational acceleration and ΔD is the vertical offset between the acoustic and pressure transducers onboard the IPS. The atmospheric pressure is acquired from nearby meteorological stations (Pelly Island, Barter Island, Point Lay) or from weather models (European Centre for Medium-Range Weather Forecasts ERA-Interim).

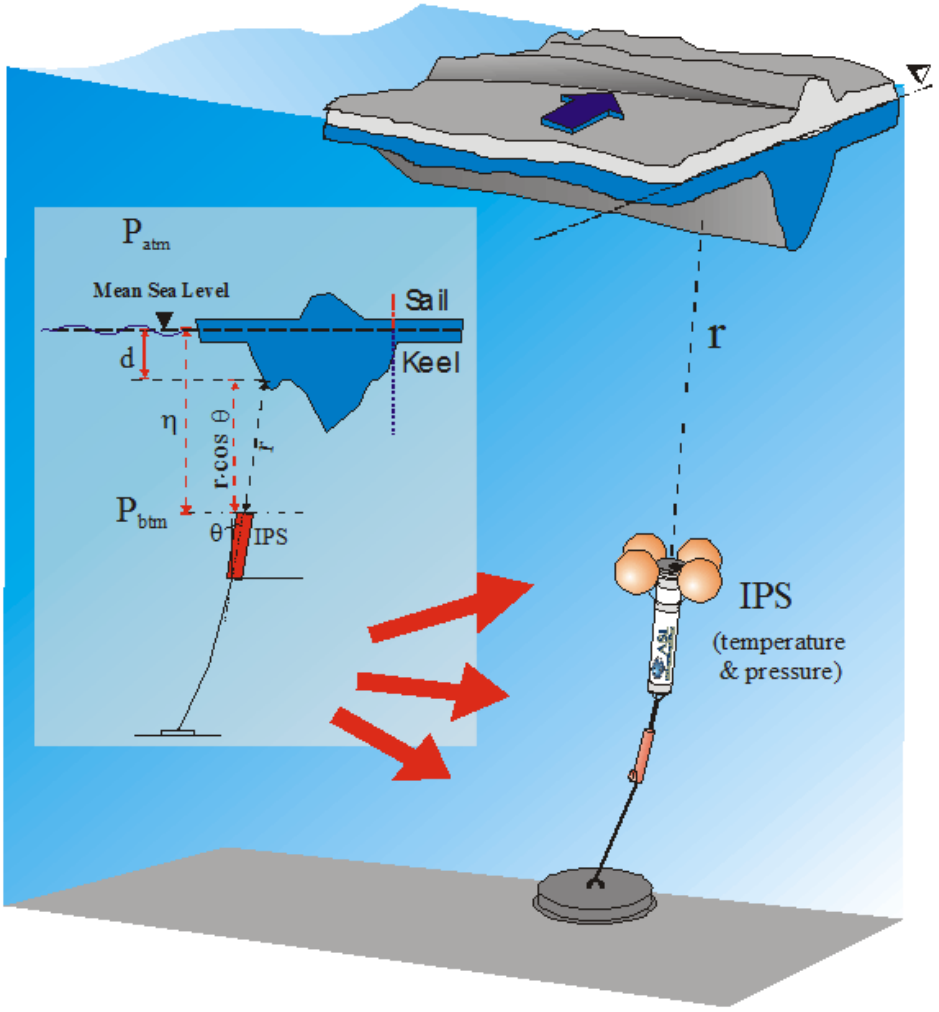

Figure 2. The ASL Ice Profiler (IPS) measures the profile of the ice under surface along the direction of ice drift.

The IPS is deployed to transmit 420 kHz pings typically at 1-2 second intervals. This leads to a high-resolution profile of the ice under surface as depicted in Figure 3 with ice drafts accurate to about 0.05 m. The ice draft time-series is subsequently transformed to an equispaced distance interval by integration with ice velocity measurements obtained by an Acoustic Doppler Current Profiler (ADCP) co-deployed within 100 m. The horizontal spatial resolution is determined by the size of the ensonified ice undercanopy; when operating at 50 m depth, the IPS-derived ice draft spatial-series has a horizontal spatial resolution of approximately 1 m. An example of the final ice draft evenly spaced in distance is shown in Figure 4 for a short segment.

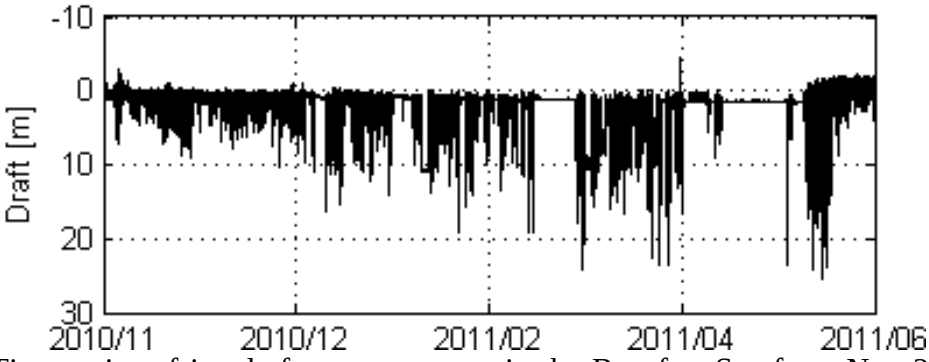

Figure 3. Time-series of ice draft measurements in the Beaufort Sea from Nov 2010 to Jun 2011.

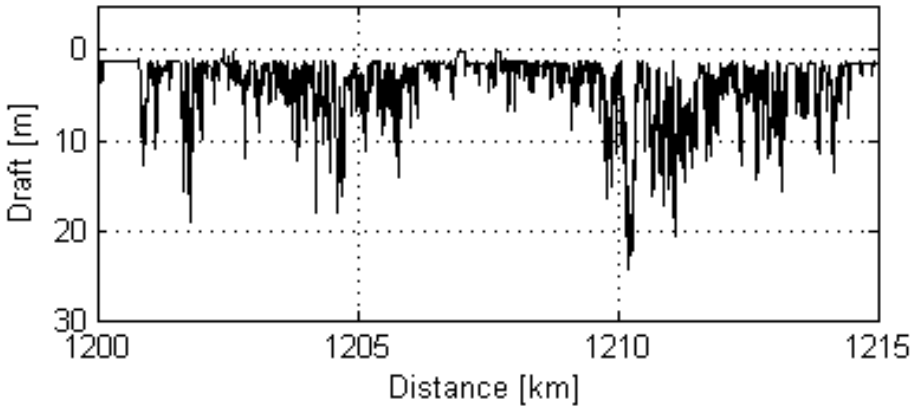

Figure 4. Ice draft measurements from the Beaufort Sea transformed to an evenly spaced distance interval determined from measurements of ice velocity.

Keel Identification

A feature detection algorithm was used to identify individual keel features within an equispaced ice draft series (Fissel et al., 2010). Three parameters characterize the algorithm:

- Start threshold – The draft value which triggers the identification of an ice keel. Forward and backward searches for the end and start of the keel, respectively, are performed from the draft data record that exceeds the start threshold.
- End threshold – The absolute minimum draft value which triggers the boundary of a keel, i.e. the start or end. This is typically set to the expected level ice draft in the region of interest determined through ice charts and ice draft time-series.
- Alpha – The Rayleigh criterion which is used to determine an adaptive draft threshold for detecting the start or end of a keel. The draft threshold, d_T, based on this parameter is calculated as:

$$d_T = (1 - \alpha) d_{max} \quad (4)$$

where d_{max} is the maximum of the draft records that comprise the keel feature.

The draft data is scanned from the beginning until a draft record exceeds the start threshold. This point establishes the current start of an individual keel. The draft data is scanned from the start of the keel while continually updating d_{max} and checking if the keel has ended by a draft record that is either less than the end threshold or less than the adaptive draft threshold and the slope has reversed. Upon finding the end of the keel, the start of the keel is found by searching backward from the current start using the same criteria as was used to find the keel end. The maximum keel draft is not updated during the backwards scan. The search results in

a list of start and end record indices that identify individual keel features from the complete draft data (Figure 5). After identifying the start and end record indices of all qualifying keel features, features that overlap are combined into a single keel. Overlaps can occur due to the changing impact of the adaptive draft threshold on the start and end points.

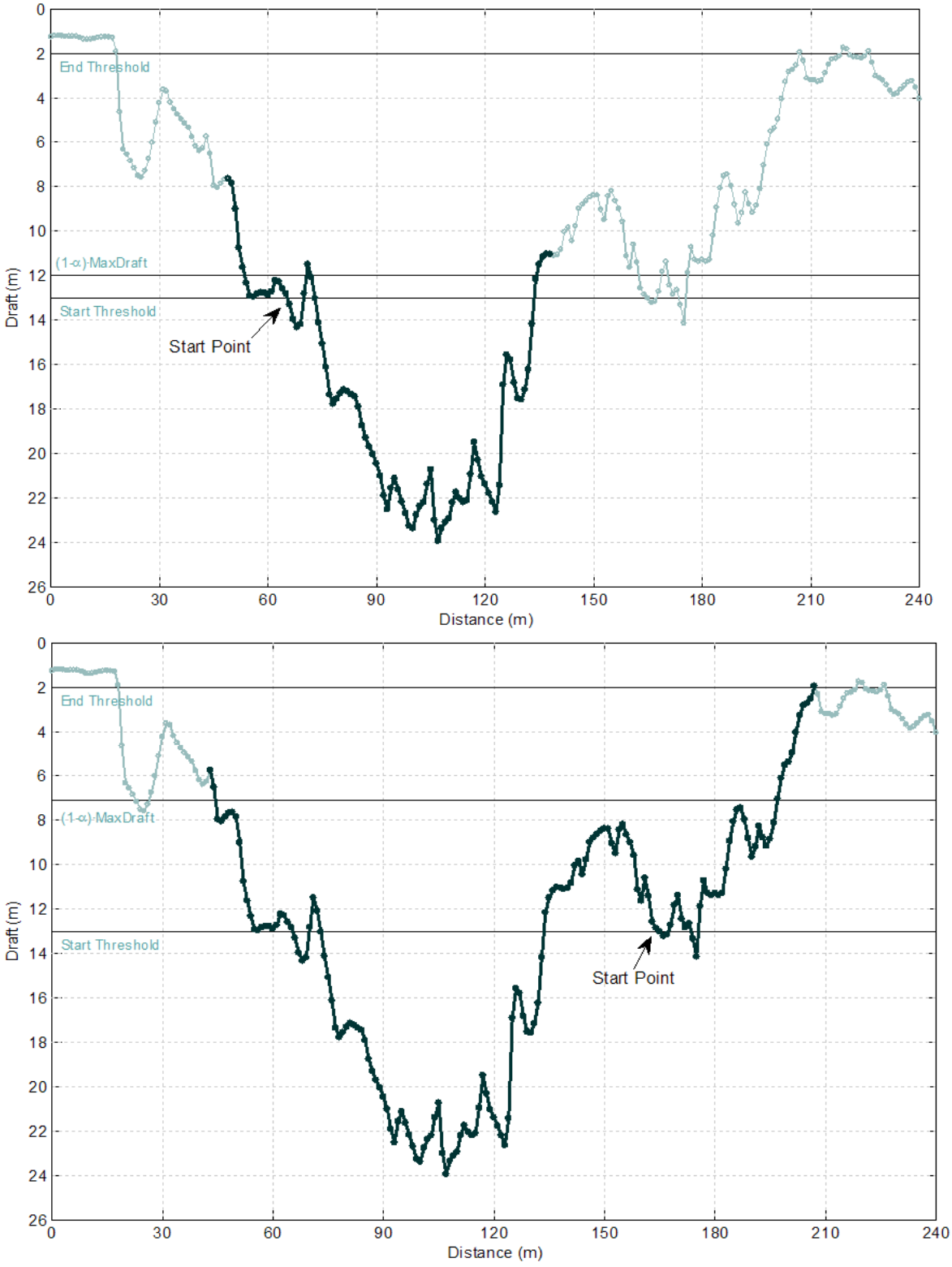

Figure 5: An example of the thresholds used by the keel feature detection algorithm (top). This particular keel was found using a 13 m start threshold, 2 m end threshold and α equal to 0.5. Any overlapping keels are combined (bottom).

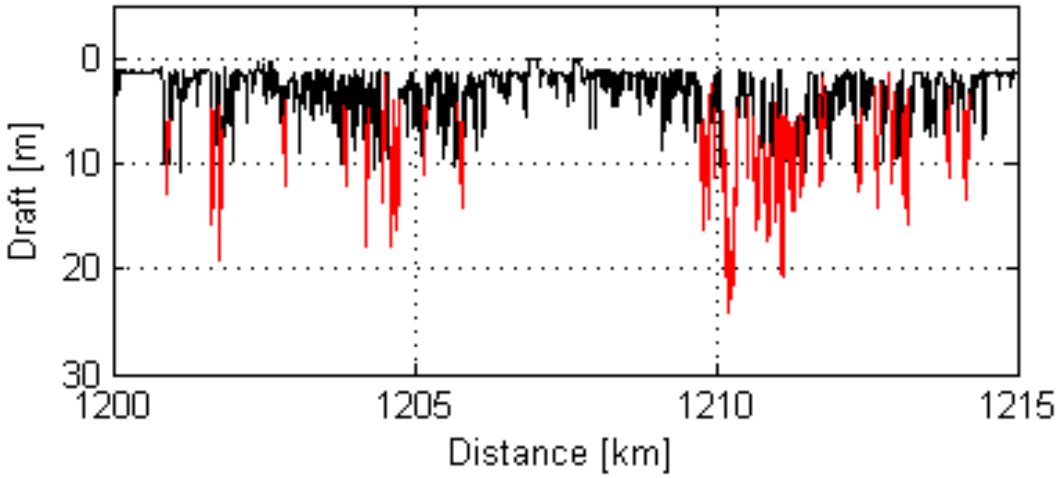

Figure 6: Ice draft measurements from the Beaufort Sea transformed to an evenly spaced distance interval with keel features identified (red).

In our analysis we used an end threshold of 2 m and a value for α of 0.5. Since we are concerned with the extreme end of the keel draft distribution we used a start threshold of 11 m. Figure 6 shows an example of the keel identification results when the detection algorithm is applied to the ice draft time-series plotted in Figure 4.

Maximum Draft vs. Level Ice Draft

An earlier analysis (Amundrud, 2004) led to an empirically determined relationship between the maximum ice draft, *d*, and the draft of nearby level ice, *h*, based on draft observations from the Beaufort Sea in the 1990s:

$$d = 20h^{1/2} \qquad (9)$$

where the variable values are expressed in metres. Amundrud et al. argued that ridging in first-year ice continues as long as the force required to drive an ice block over the ridge is less than the force at which the level ice next to the ridge will buckle.

We performed a similar empirical analysis on recent draft observations from the Beaufort Sea, Fram Strait, Chukchi Sea and Camden Bay. The equispaced ice draft records were divided into 50 km segments. For each segment the following procedure was used:

- The maximum draft of each segment was found and its distance location was recorded.
- The draft data within 5 km of the maximum draft was extracted.
- A histogram of the extracted draft data segment was calculated using 0.2 m bins.
- The mode of the draft distribution was found by selecting the bin containing the maximum number of data values.
- The median of the data values in the selected bin and its two neighbouring bins was calculated and this was determined to be the level ice draft in the region of the maximum draft event.

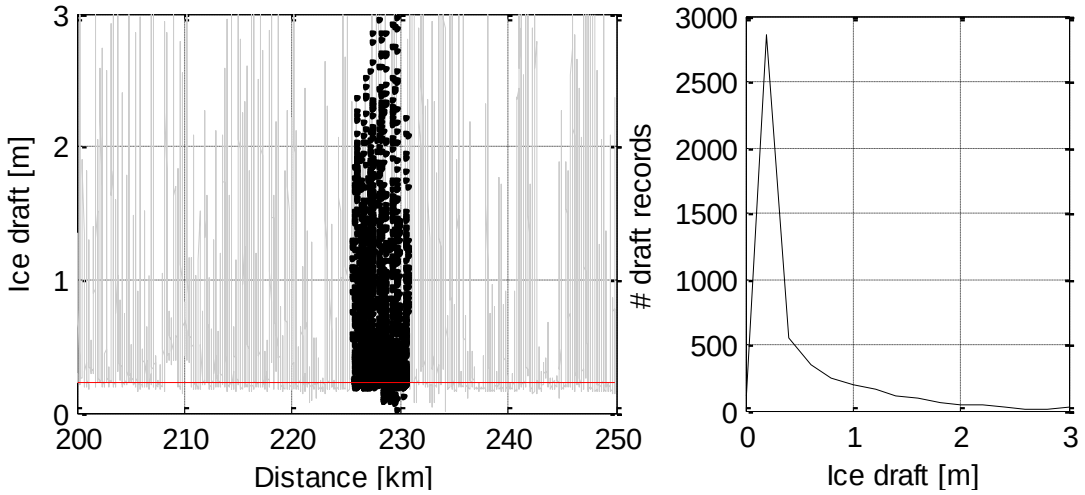

Figure 7: An example of the determination of the level ice draft (red) in the segment of data near the maximum draft (black) of a 50 km segment of equispaced ice draft (grey). The righthand plot shows the draft distribution of the black data values.

An example of this process is shown in Figure 7. The 50 km draft segment is plotted in grey with the 5 km sub-segment of draft values about the maximum draft shown with black markers. The histogram of the draft values in the sub-segment is shown on the right. The level ice draft derived from the median of the data values in the bin corresponding to the maximum of the histogram is shown plotted in red.

RESULTS

Very Large Ice Keels

The keel detection algorithm described above was used to detect individual keel features that exceed 11 m in maximum ice draft. This resulted in thousands of identified features as listed in Table 1. The frequency of occurrence of these very large ice keels varies considerably from one measurement site, by up to a factor of two within a region, as seen in Table 1 for the Fram Strait region and by lesser amounts in other regions. Very large differences also occur between the regions, with the Fram Strait area off NE Greenland having the largest number of 11 m ice keels which exceeds those of other regions by a factor of two. The numbers in the shelf region of the Canadian Beaufort Sea are notably reduced (Table 1) from those off Camden Bay of the Eastern Alaskan Beaufort Sea Shelf and the Chukchi Sea shelf areas.

Table 1: A summary of the sets of keel results used in this study given by the region and years over which they were observed, the number of 11 m keels observed at each site with the site-years in parentheses (i.e. the sum of the number of measurement sites by year), the total number of keels and the average number of keels observed at each site and the average number of keels in each 100 km of observed ice.

Region	Deployment years	Number of identified keels (site-years)					Total per site year	Total per unit length [keel/100 km]
		Site 1	Site 2	Site 3	Site 4	Total		
Canadian Beaufort Sea	1999-2011	2621 (9)	1818 (7)	-	-	4439 (16)	277	14.4
Fram Strait	2008-2009	1213 (1)	2224 (1)	-	-	3437 (2)	1719	30.3
Camden Bay	2005-2012	7603 (7)	3172 (5)	-	-	10775 (12)	898	48.0
Chukchi Sea	2009-2012	3427 (4)	803 (1)	2379 (3)	2542 (3)	9151 (11)	832	33.0

Maximum Draft vs. Level Ice Draft

Table 2 lists for each measurement site the number of 50 km transects analysed for the maximum draft event and the corresponding draft of the nearby level ice. The total set of results are scatter plotted to show the relationship between maximum and level ice draft in Figure 8 which clearly shows a large number exceeding the truncation curve. The number of transects with corresponding results above the curve range between the analysis regions from about 14 to 35 per cent of the total transects analysed (Table 2). The majority of these are likely related to the presence of multi-year ice. The keels of old or multi-year ice have been generated in previous years rather than recently in association with the undeformed local ice cover as is the case for first year ice keels. In the Amundrud analysis, ridges generated by multi-year ice were manually identified and filtered resulting in only 4 per cent of results above the truncation curve. The effect of multi-year ice is largest in the Fram Strait results where this ice type is more prevalent due to the outflow of older ice the Arctic Ocean via Fram Strait by comparison with the western Arctic Ocean in the Beaufort and Chukchi Seas (Wadhams, 1980).

Table 2: The number of 50 km transects analysed at each measurement site.

Region	50 km transects		
	Total #	# > truncation curve	% > truncation curve
Canadian Beaufort Sea	616	98	15.9
Fram Strait	227	78	34.4
Camden Bay	449	105	23.4
Chukchi Sea	555	77	13.9

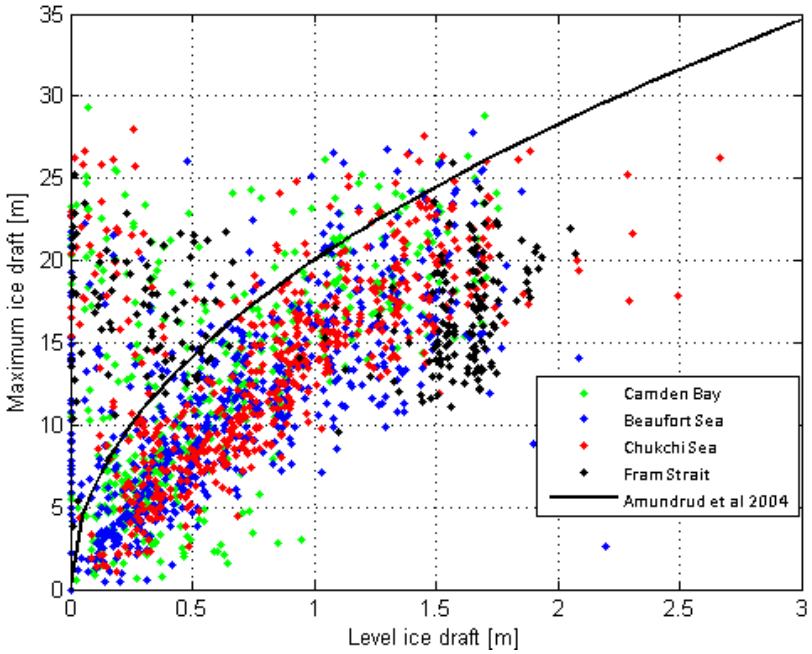

Figure 8. A comparison of the maximum draft vs. level ice draft observations for all analysed regions against the Amundrud truncation curve.

The maximum and level ice draft pair contributions can be seen more clearly for each region in Figure 9. The Camden Bay, Beaufort Sea and Chukchi Sea results are largely bounded by the truncation curve and comprise the full domain of expected level ice draft values from the early growth of thin ice to the maximum undeformed ice draft of about 2.5 m. The Fram Strait results differ significantly with the majority of the results below 1 m of level ice draft lying above the truncation curve. The Fram Strait ice draft distributions were observed to be

strongly bi-modal and the analysis algorithm often selected the mode corresponding to the shallower ice draft. If the detected maximum ice drafts were actually generated by the undeformed ice sheet corresponding to the deeper ice draft mode, the points above the truncation curve would move to the right potentially below the curve. The presence of multi-year ice is also certainly confounding the Fram Strait results and potentially situating deep keel features in thin undeformed ice that was not a participant in their genesis. Glacial ice features, also known to be present off the east coast of Greenland, may also contribute to the outlier points noted in Figure 9.

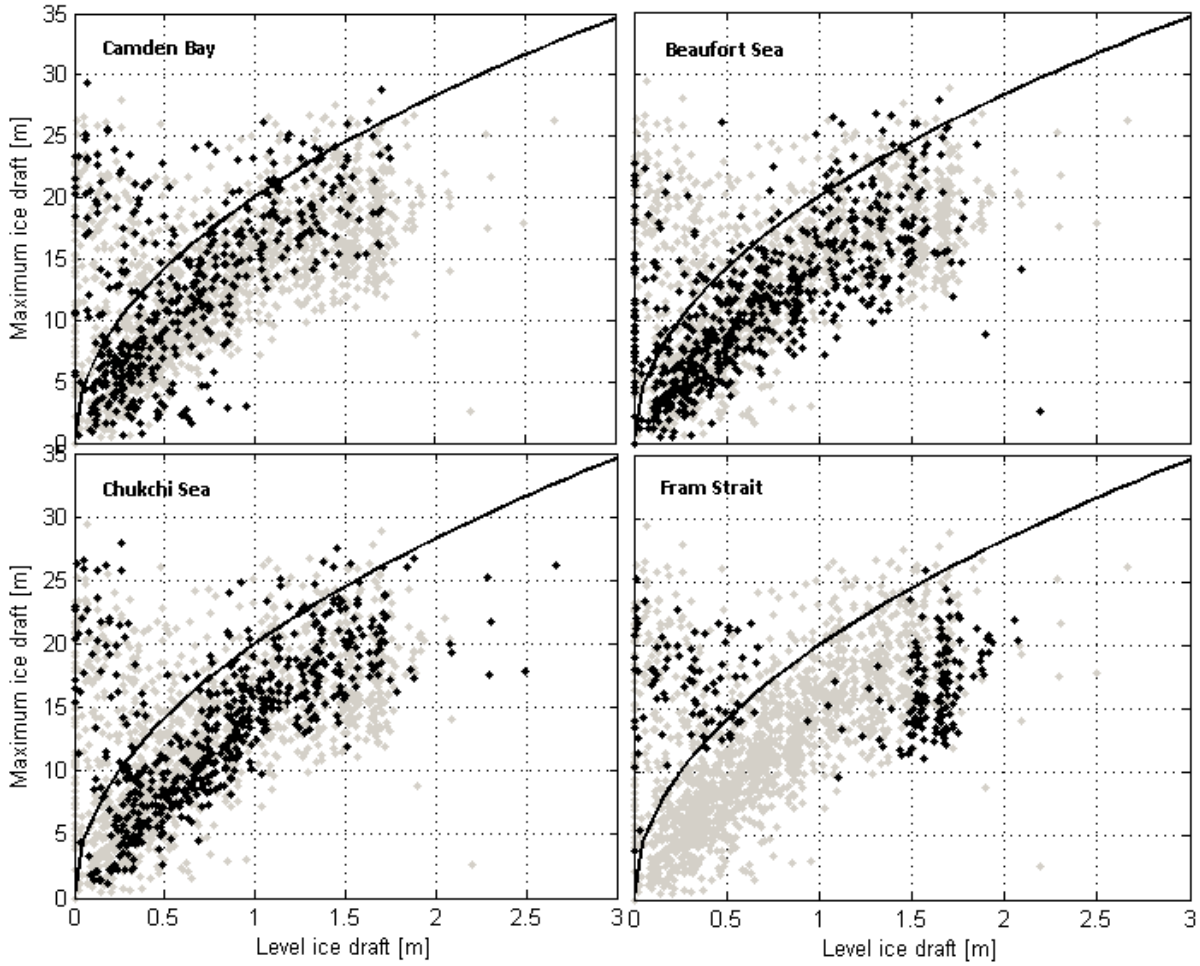

Figure 9. A comparison of the maximum draft vs. level ice draft observations by region.

Multi-year Ice

The ice regimes of the regions analysed in this paper differ significantly in terms of the frequency of occurrence of the largest ice keels. While the composition of Arctic ice has undergone dramatic changes in recent yearsa key differentiator between these regions – the abundance of multi-year ice – has persisted. As shown in Figure 10, the ice regime in the shelf regions of the Beaufort Sea and Chukchi Sea mainly now consists of first and second year ice. The presence of older ice is very low in the shelf areas, while a large amount of third year and older ice passes through Fram Strait in both the shelf and slope regions.

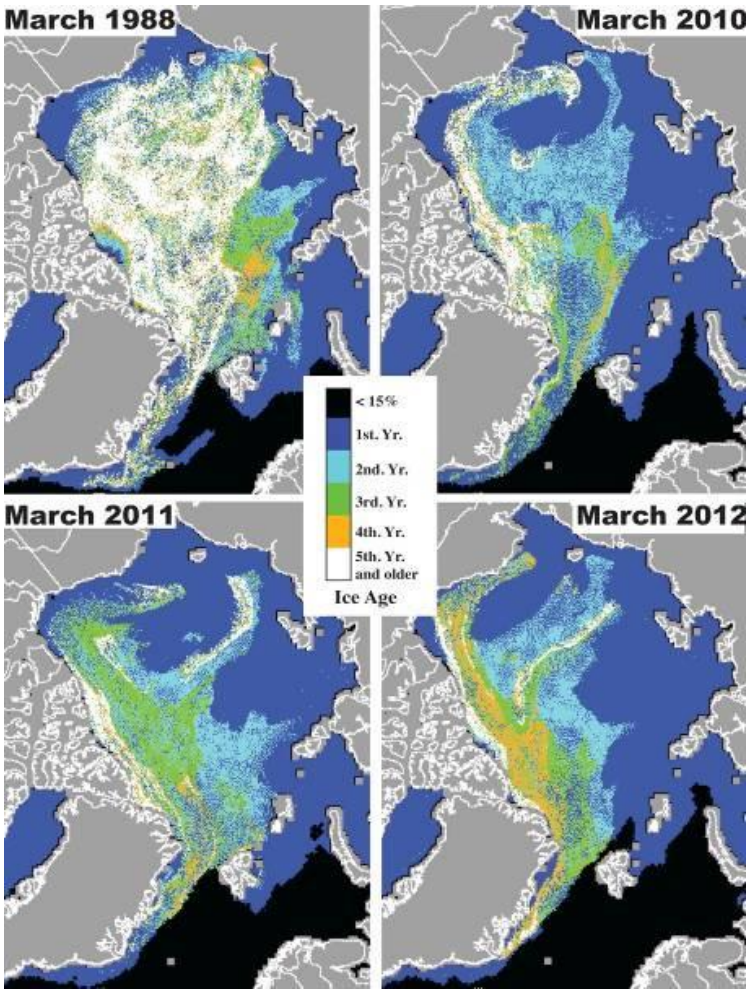

Figure 10. The development of sea ice age over time showing a decrease in multi-year ice in the Chukchi and Beaufort Seas and a predominance of multi-year ice in Fram Strait (Perovich et al., 2012).

The automated detection of multi-year ice, and also glacial ice, from upward looking sonar data sets would lead to being able to differentiate the marine ice populations according to their underlying characteristic types: first year ice, old and multi-year ice, and glacial ice. Progress is being made in developing algorithms for this purpose (Fissel et al., 2012).

CONCLUSIONS

Two types of analysis were used to develop understandings of the extreme marine ice drafts by different geographical regions within the Arctic Ocean from many year-long upward looking sonar data sets.

The first analysis involves a keel detection algorithm used to detect very large individual keel features within the high resolution upward looking sonar measurements of ice draft vs. distance travelled by the ice. For this application, very large individual ice keels that exceed 11 m in maximum ice draft were identified. The frequency of occurrence of these very large ice keels varies considerably from one measurement site, by up to a factor of two within a region. Very large differences also occur between the regions, with the Fram Strait area off NE Greenland having the largest number of 11 m ice keels which exceeds those of other regions by a factor of two. The numbers of the very large ice keel features in the shelf regions

of the Canadian Beaufort Sea are notably reduced from those off Camden Bay of the Eastern Alaskan Beaufort Sea Shelf and the Chukchi Sea shelf areas.

The second analysis found an empirically determined maximum draft upper bound which constrains the majority of observations of maximum ice draft features and corresponding nearby level ice draft. Observations beyond this curve are likely due to misclassification. More Fram Strait observations are necessary to assess the results of this analysis in that ice regime; however, it is evident that the effects of multi-year ice are abundant even in the relatively shorter data record.

Recent research into the use of the Ice Profiler to detect multi-year ice shows promising direction (Fissel et al., 2012). As this capability improves, the dissection of ice feature observations into age classifications will affect the analyses discussed in this paper and ultimately lead to improved estimates of extreme and hazardous ice features of different kinds.

ACKNOWLEDGEMENTS

The authors wish to thank Dr. Humfrey Melling (Department of Fisheries and Oceans, Institute of Ocean Sciences), Dr. Edmond Hansen (Norwegian Polar Institute), Shell and ConocoPhillips for allowing the use of the upward looking sonar data for this study.

REFERENCES

Amundrud, T. L. 2004. Geometrical constraints on the evolution of ridged sea ice. *Journal of Geophysical Research,* 109.

Fissel, D.B., J.R. Marko and H. Melling, 2008. Advances in upward looking sonar technology for studying the processes of change in Arctic Ocean ice climate. Journal of Operational Oceanography: 1(1), 9-18.

Fissel, D., Ross, E., Borg, K., Billenness, D., Kanwar, A., Bard, A., Sadowy, D. & Mudge, T. 2012. Improvements in the Detection of Hazardous Sea Ice Features Using Upward Looking Sonar Data. *Artic Technology Conference 2012.* Houston, TX.

Fissel, D. B., Kanwar, A., Borg, K., Mudge, T., Marko, J. R. & Bard, A. Automated Detection of Hazardous Sea Ice Features from Upward Looking Sonar Data. Icetech, 2010 Anchorage, Alaska, USA.

Perovich, D., Meier, W., Tschudi, M., Gerland, S. & Richter-Menge, J. 2012. Sea Ice. *Arctic Report Card 2012*.

Ross, E., Fissel, D., Marko, J. R. & Reitsma, J. 2012. An Improved Method of Extremal Value Analysis of Arctic Sea Ice Thickness Derived From Upward Looking Sonar Ice Data. *Arctic Technology Conference 2012.* Houston, TX.

Wadhams, P.. 1980. Ice in the Ocean. *Gordon and Breach, Amsterdam,* 351 p.